Heat and Mass Transfer to Spheres at Low Reynolds Numbers and High Mass Transfer Rates

G. M. FAETH
Pennsylvania State University, University Park, Pennsylvania

During the evaporation and condensation of droplets in the presence of a noncondensible gas, there can be no net flux of the noncondensible gas at the droplet surface. This gives rise to a bulk velocity to oppose the diffusion of the noncondensible gas. This diffusion-induced velocity affects the overall heat and mass transfer rates of the droplet, particularly at high mass transfer rates where the velocity is large. Fuchs (*1*) has determined the necessary corrections for the presence of this velocity for a motionless droplet, but similar information is lacking for moving droplets. This problem is considered in the following for the low Reynolds number regime.

The diffusion-induced velocity is proportional to the radial concentration gradient at the surface of the droplet. For a moving droplet this gradient varies over the droplet surface, causing a similar variation in the induced velocity. However, we would expect that this variation is not large at low Reynolds numbers, and as a first approximation we consider the case of a uniform radial velocity at the droplet surface. It is also assumed that the gas is incompressible and that the properties of all species are the same and are constant throughout the flow field. Under these assumptions the nondimensional transport equation for the region around the sphere has the following form:

$$\mathcal{V}_r \frac{\partial \psi}{\partial \eta} + \frac{\mathcal{V}_\theta}{\eta}\frac{\partial \psi}{\partial \theta} = \frac{2}{N_{Pe}}\frac{1}{\eta^2}\left[\frac{\partial}{\partial \eta}\left(\eta^2 \frac{\partial \psi}{\partial \eta}\right) + \frac{\partial^2 \psi}{\partial \theta^2} + \cot\theta \frac{\partial \psi}{\partial \theta}\right] \quad (1)$$

ψ and N_{Pe} have different meanings depending upon the process being considered. For heat transfer

$$\psi = \frac{T - T_o}{T_\infty - T_o}, \quad N_{Pe} = N_{Re} \times N_{Pr} \quad (2)$$

and for binary mass transfer where W is the mass fraction of the evaporating or condensing material

$$\psi = \frac{W - W_o}{W_\infty - W_o}, \quad N_{Pe} = N_{Re} \times N_{Sc} \quad (3)$$

The boundary conditions for both cases are

$$\eta = 1 \;\; \psi = 0, \quad \eta \to \infty \;\; \psi = 1 \quad (4)$$

By exploiting the linearity of the momentum equation at low Reynolds numbers, we can obtain the velocities in Equation (1) by superimposing the Stokes solution and the spherically symmetric radial flow resulting from the surface velocity. With θ measured from the forward stagnation point, the velocities are

$$\mathcal{V}_r = A - B\cos\theta$$
$$\mathcal{V}_\theta = C\sin\theta \quad (5)$$

where, if $\mathcal{V}_{ro}$ is the surface velocity

$$A = \mathcal{V}_{ro}/\eta^2$$
$$B = 1 - \frac{3}{2}\frac{1}{\eta} + \frac{1}{2}\frac{1}{\eta^2}$$
$$C = 1 - \frac{3}{4}\frac{1}{\eta} - \frac{1}{4}\frac{1}{\eta^2} \quad (6)$$

The solution of Equation (1) subject to Equations (4), (5), and (6) was obtained by a method suggested by Yuge (*2*) and employed as well by Pfeffer and Happel (*3*) in transport studies of spheres at low Reynolds numbers. This involves expanding ψ in even powers of θ with coefficients that are functions of η alone

$$\psi = f_o(\eta) + f_2(\eta)\theta^2 + f_4(\eta)\theta^4 + \ldots \quad (7)$$

As a first a pproximation, $\sin\theta$ and $\cos\theta$ are expanded in powers of θ and the derivatives with respect to θ on the right-hand side of Equation (1) are neglected. By equating like powers of θ we obtain an infinite set of ordinary differential equations, the first three of which are

$$f_o'' + \left[\frac{2}{\eta} + \frac{N_{Pe}}{2}(B - A)\right] f_o' = 0$$

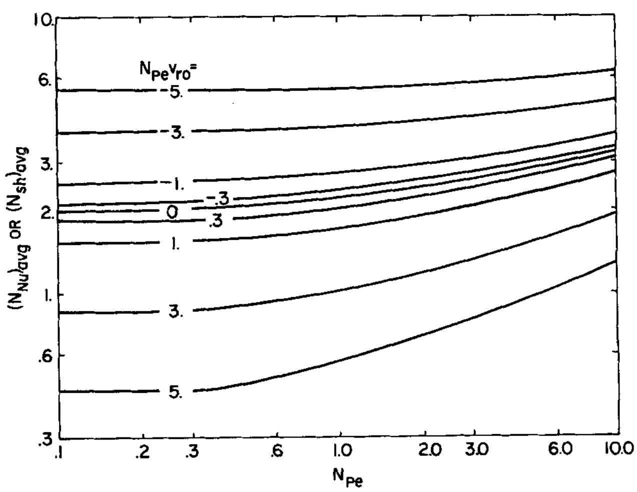

Fig. 1. Nusselt or Sherwood numbers for spheres at various transfer rates.

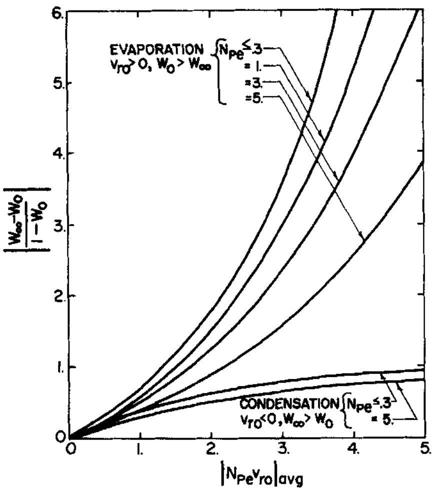

Fig. 2. Mass fraction ratio as a function of surface velocity.

$$f_2'' + \left[\frac{2}{\eta} + \frac{N_{Pe}}{2}(B-A)\right]f_2' - \frac{N_{Pe}C}{\eta}f_2 = \frac{N_{Pe}B}{4}f_o'$$

$$f_4'' + \left[\frac{2}{\eta} + \frac{N_{Pe}}{2}(B-A)\right]f_4' - \frac{2N_{Pe}C}{\eta}f_4 = \frac{N_{Pe}B}{2}\left(\frac{f_2}{2!} - \frac{f_o}{4!}\right) - \frac{N_{Pe}C}{3!}\frac{f_2}{\eta} \quad (8)$$

with boundary conditions

$$f_o = f_2 = f_4 = .. = 0 \quad \eta = 1,$$
$$f_o = 1 \quad f_2 = f_4 = .. = 0 \quad \eta = \infty \quad (9)$$

A second approximation is obtained by letting

$$\psi = g_o(\eta) + g_2(\eta)\theta^2 + g_4(\eta)\theta^4 + \ldots. \quad (10)$$

and by substituting the first approximation into the term that was omitted in Equation (1). When we proceed as before, a second set of differential equations is obtained, the first of which is

$$g_o'' + \left[\frac{2}{\eta} + \frac{N_{Pe}}{2}(B-A)\right]g_o' = -\frac{4}{\eta^2}f_2 \quad (11)$$

with boundary conditions analogous to Equation (9). Further approximation may be obtained in a similar manner.

By defining heat and mass transfer coefficients as

$$h = \frac{k\left(\frac{\partial T}{\partial r}\right)_{r=a}}{T_\infty - T_o} \qquad K = \frac{\rho D\left(\frac{\partial W}{\partial r}\right)_{r=a}}{W_\infty - W_o} \quad (12)$$

and by expressing these equations in dimensionless form we obtain the following for the second approximation:

$$N_{Nu}(\text{or } N_{Sh}) = 2[g_o' + g_2'\theta^2 + g_4'\theta^4 + \ldots]_{\eta=1} \quad (13)$$

The average value of the Nusselt number is found by integrating Equation (13) over the sphere with the result

$$(N_{Nu})_{avg} = [2g_o' + (\pi^2 - 4)g_2' + (\pi^4 - 12\pi^2 + 48)g_4' + \ldots]_{\eta=1} \quad (14)$$

The numerical solution of these equations was obtained by the Runge-Gill procedure coupled with trial and error matching of the boundery conditions. It was found that the Nusselt numbers obtained from Equation (14) and those calculated by replacing g_2' and g_4' with f_2' and f_4' were essentially identical, so the latter procedure was employed in the bulk of the calculations.

Figure 1 is a plot of average Nusselt or Sherwood number vs. N_{Pe} with $N_{Pe}\mathcal{V}_{ro}$ as a parameter. Negative values of $N_{Pe}\mathcal{V}_{ro}$ occur for condensation, while positive values represent evaporation. As N_{Pe} becomes small the values approach the well-known result for a motionless sphere

$$(N_{Nu})_{avg} = \frac{N_{Pe}\mathcal{V}_{ro}}{\exp\left(\frac{N_{Pe}\mathcal{V}_{ro}}{2}\right) - 1}, \quad N_{Pe} \to 0 \quad (15)$$

The numerical calculations essentially give this value for $N_{Pe} \leqq 0.3$.

The condition of no net flux of the noncondensible gas at the droplet surface is formulated as

$$N_{Pe}\mathcal{V}_{ro} = -\left(\frac{W_\infty - W_o}{1 - W_o}\right)N_{Sh} \quad (16)$$

By taking averages of both sides of Equation (16) and by employing the previous results giving the Sherwood number as a function of $N_{Pe}\mathcal{V}_{ro}$ and N_{Pe}, we obtain a relationhip between the surface velocity and the surface concentration of the diffusing species. This is illustrated in Figure 2 for various values of N_{Pe} both for evaporation and condensation.

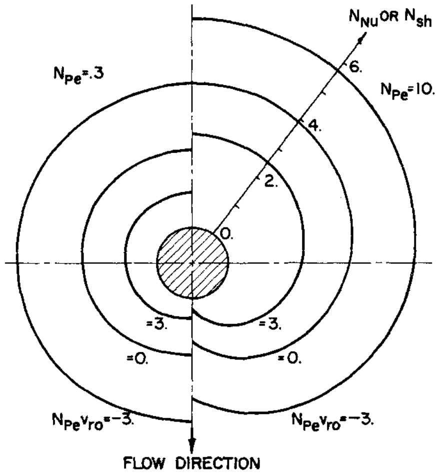

Fig. 3. Distribution of local Nusselt or Sherwood numbers around the sphere.

The variation of the local Nusselt or Sherwood number around the sphere is shown in Figure 3 for various values of N_{Pe} and $N_{Pe}\mathcal{V}_{ro}$. If we assume as a second approximation that the actual distribution of $\mathcal{V}_{ro}$ is given by Equation (16), the results of Figure 3 show that the surface velocity distribution becomes less uniform at high values of N_{Pe} and $N_{Pe}\mathcal{V}_{ro}$. Further study is required to determine where this variation introduces significant errors in the transport coefficients given by the present analysis.

NOTATION

a = sphere radius, ft.

A, B, C = functions of η defined by Equation (6), dimensionless

C_p = specific heat of fluid, B.t.u./(lb.) (°F.)

D = mass diffusivity, sq. ft./hr.

f_o, f_2, f_4 = functions of η defined by Equation (7), dimensionless

g_o, g_2, g_4 = functions of η defined by Equation (10), dimensionless

h = heat transfer coefficient, B.t.u./(sq.ft.) (hr.) (°F.)

K = mass transfer coefficient, lb./(sq.ft.) (hr.)

k = thermal conductivity of fluid, B.t.u./(hr.) (ft.) (°F.)

N_{Nu} = Nusselt number = $2ah/k$, dimensionless

N_{Pe} = Peclet number = $N_{Re} \times N_{Pr}$ or $N_{Re} \times N_{Sc}$, dimensionless

N_{Pr} = Prandtl number $= C_p\mu/k$, dimensionless

N_{Re} = Reynolds number = $2a\rho U/\mu$, dimensionless

N_{Sc} = Schmidt number = $\mu/\rho D$, dimensionless

N_{Sh} = Sherwood number = $2aK/\rho D$, dimensionless

r = radial distance, ft.

T = temperature, °F.

U = velocity of undisturbed flow, ft./hr.

$\mathcal{V}_r$ = dimensionless radial velocity $= V_r/U$

$\mathcal{V}_\theta$ = dimensionless velocity in the θ direction $= V_\theta/U$

V_r = radial velocity, ft./hr.

V_θ = velocity in the θ direction, ft./hr.

W = mass fraction of the diffusing species, dimensionless

Greek Letters

α = thermal diffusivity, sq.ft./hr.

η = dimensionles radial distance = r/a

θ = angle measured from forward stagnation point, rad.

μ = viscosity of fluid, lb./(ft.) (hr.)

π = 3.14159 . . . . . , dimensionless

ρ = density of fluid, lb./cu.ft.

ψ = dimensionless temperature or mass fraction = $T - T_o/T_\infty - T_o$ or $W - W_o/W_\infty - W_o$

Subscripts

o = at surface of sphere ($r = a$)

∞ = far from sphere ($r \rightarrow \infty$)

LITERATURE CITED

1. Fuchs, N., *Natl. Advisory Comm. Aeronaut. Tech. Mem. 1160* (1947).
2. Yuge, T., *Rept. Inst. High Speed Mechanics Tohoku Univ.*, **6**, 143 (1956).
3. Pfeffer, R., and John Happel, *A.I.Ch.E. J.*, **10**, 611 (1964).

Inconsistency in the Transfer Analogies

EDWARD H. LEBEIS, JR.

Media, Pennsylvania

The Colburn analogy (*3*) for heat transfer and the Chilton-Colburn analogy (*2*) for mass transfer have provided a useful framework for the correlation of transfer coefficients. However, the success of these analogies with fluid friction has not been unqualified, since different investigators working with the same system have defined different lines on a plot of j factor and friction factor vs. Reynolds number. The purpose of this discussion is to point out a fundamental inconsistency in the analogies which may explain their partial failure.

The friction factor plot upon which the analogy is graphically based represents the frictional loss in terms of number of velocity head per unit dimensionless length (L/D). It applies only to the pressure drop in tubes at a considerable distance from the inlet of the tube. Prandtl and Tietjens (*12*) have shown that the friction factor plot can be constructed from Hagen's (*6*) pressure drop data for the entire pipe (from supply tank to outlet), provided the abnormally high entrance pressure drop is subtracted. The subtraction amounts to 2.7 velocity heads in laminar flow, and 1.4 velocity heads in turbulent flow.

In each case, one velocity head represents the gain in kinetic energy achieved by the acceleration of the fluid from zero velocity in the supply tank to the mean velocity in the tube. The remainder represents the extra pressure loss associated with the establishment of the final form of the velocity profile. After calculating pressure drop in a tube with the aid of the friction factor plot, one adds the appropriate "entrance loss."

The accepted concept of no-slip at the tube wall requires a shear stress at the tube entrance approaching infinity, since the fluid near the wall must decelerate from a finite velocity to a velocity approaching zero. The work of Deissler (*4*) has shown that the friction factor does indeed approach infinity at the tube entrance and that it decreases toward a constant terminal value as the distance from the inlet increases. If the tube is sufficiently long, the integral value of the "extra" pressure drop should be equivalent to the entrance loss mentioned above.

If heat or matter is being transferred at the tube wall, an analogous situation exists. At the tube entrance, heat or matter is transferred to fluid elements closest to the tube wall through a distance approaching zero, so the transfer coefficient approaches infinity. The coefficient declines toward a constant terminal value as the tube length increases and the mean distance for transfer increases toward an asymptotic value. This aspect is discussed in considerable detail elsewhere (*8*).

LAMINAR FLOW

For the case of heat transfer with laminar flow in a short cylindrical conduit with constant wall temperature, parabolic velocity distribution established, and invariant properties, Colburn (*3*) converted Lévêque's (*9*) equation

$$\frac{h_a}{\rho c_p} = 1.615 \left(\frac{\alpha^2 \bar{u}}{DL} \right)^{1/3}$$

$$= 1.615 \left(\frac{\alpha^2}{D\theta} \right)^{1/3} \quad (1)$$

to the form

$$j = N_{St} N_{Pr}^{2/3} = 1.615\, N_{Re}^{-2/3} \, (L/D)^{-1/3} \quad (2)^*$$

Lévêque's equation predicts an infinite value for the coefficient at the start of the heated length ($L = 0$) and a continuous decrease in coefficient with increase in heated length. If heat transfer were started at the tube inlet, where the velocity distribution approaches uniformity, the heat transfer analog of Higbie's equation would apply for a very short distance, again predicting an infinite coefficient.

As discussed by Norris and Streid (*10*) it is regrettable that h_a, the arithmetic mean coefficient, was chosen for the analogy. Lévêque also showed that h_M, the coefficient based on log mean temperature difference, is defined for short tubes by the same equation as above for the coefficient based on arithmetic mean Δt.

Lévêque further showed that, unlike h_a, the log mean coefficient approaches a constant terminal value, which can be expressed in the form

$$\text{Minimum Nusselt number} = 3.66 \quad (3)$$

This terminal value is in complete accord with Graetz's (*5*) precise infinite series solution to the problem, which does not depend on the assumption of a short heated length.

Since the friction factor plot excludes the inlet behavior and gives only the terminal "coefficient" for momentum

* The numerical constant in Colburn's paper does not agree with that given by Lévêque.